Crystal and Lamella Structure and C−H···O═C Hydrogen Bonding of Poly(3-hydroxyalkanoate) Studied by X-ray Diffraction and Infrared Spectroscopy

Harumi Sato,*,†,‡ Katsuhito Mori,†,‡ Rumi Murakami,†,‡ Yuriko Ando,†,‡ Isao Takahashi,†,‡ Jianming Zhang,†,‡ Hikaru Terauchi,†,‡ Fuminobu Hirose,§ Kenichi Senda,§ Kohji Tashiro,⊥,‡ Isao Noda,‡,# and Yukihiro Ozaki†,‡

School of Science and Technology and Research Center for Environment Friendly Polymers, Kwansei-Gakuin University, Sanda 669-1337, Japan; Polymer Designing and Processing Research Laboratories, Kaneka Corporation, Settsu 566-0072, Japan; Department of Future Industry-oriented Basic Science and Materials, Graduate School of Engineering, Toyota Technological Institute, Hisakata, Tempaku, Nagoya 468-8511, Japan; and The Procter & Gamble Company, 8611 Beckett Road, West Chester, Ohio 45069

Received August 11, 2005; Revised Manuscript Received December 14, 2005

ABSTRACT: Temperature-dependent X-ray diffraction and infrared (IR) spectra were measured for poly(3-hydroxybutyrate) (PHB) and poly(3-hydroxybutyrate-*co*-3-hydroxyhexanoate) P(HB-*co*-HHx) (HHx = 2.5, 3.4, 10.5, and 12 mol %) to explore their crystal and lamella structure and the C−H···O═C hydrogen bonding in them. The X-ray diffraction and IR measurements of PHB and P(HB-*co*-HHx) revealed that the smaller the *a* lattice parameter, the higher the frequency (∼3008 cm^{-1}) of the C−H stretching band of the C−H···O═C hydrogen bonding along the *a* axis between the CH_3 group of one helix and the C═O group of another helix. Therefore, it seems that the C−H···O═C hydrogen bonding becomes strong with the decrease in the *a* lattice parameter. To investigate the relation between the C−H···O═C hydrogen bonding and the lamella structure, we estimated the number of C−H···O═C hydrogen bonding along the *c* axis (the direction of the lamella thickness) based on the reported lamella thickness. It is about 8 or 9 for PHB and about 3 for P(HB-*co*-HHx) (HHx = 10.5 and 12 mol %). It is very likely that the C−H···O═C hydrogen bondings break much more easily in P(HB-*co*-HHx) than in PHB because of the bulkiness of large amounts of amorphous parts. However, the polymer chains still keep the lamella structure even in the copolymers with the HHx content of more than several percent. This is the reason why the P(HB-*co*-HHx) copolymers show high crystallinity and essentially have the same lattice spacing as the PHB homopolymer even if the HHx content is more than 10%. We have concluded that the C−H···O═C hydrogen bonding stabilizes the chain folding in the lamella structure of PHB and P(HB-*co*-HHx) and the high crystallinity of PHB and P(HB-*co*-HHx) partly comes from the C−H···O═C hydrogen bonding.

Introduction

Poly(3-hydroxybutyrate) (PHB) is well-known as a biosynthesized aliphatic polyester and also a biodegradable thermoplastic.[1−10] Since the first discovery of PHB in 1920s,[1] its biosynthesis mechanism, biodegradation mechanism, crystal structure, and physical properties have been matters of extensive studies.[2−10] PHB has a perfectly isotactic structure with only *R* configuration. PHB is an attractive polymer, but it has a few serious problems from the viewpoint of industrial applications. For example, PHB is rigid and stiff because of high crystallinity arising from the high stereoregularity of biologically produced macromolecules. Moreover, PHB is also thermally unstable during the conventional melt processing due to the high melt temperature. To reduce the excess crystallinity and improve the overall physical properties of PHB, other monomers are sometimes copolymerized with PHB.[9−13] The PHB-based copolymers such as poly(3-hydroxybutyrate-*co*-3-hydroxyhexanoate) (P(HB-*co*-HHx)) show a wide range of improved physical properties depending on the chemical structure of the comonomer units as well as the comonomer composition. Figure 1 compares chemical structures of PHB and P(HB-*co*-HHx). The biodegradation mechanism, chemical synthesis, and mechanical properties of P(HB-*co*-HHx) have been studied by several research groups.[9−13]

The crystalline structure of PHB consists of an orthorhombic system $P2_12_12_1$-D^4_2 with $a = 5.76$ Å, $b = 13.20$ Å, and $c = 5.96$ Å (fiber repeat).[14,15] Recently, on the basis of the molecular weight studies on depolymerase-treated single crystals of PHB, Marchessault et al.[16,17] suggested that the PHB single crystals create a multiple erosion surface in the fold plane direction, i.e., parallel to the long axis (*a* axis of unit cell). They suggested that the antiparallel chain packing of PHB, which provides a relatively stable tubular ribbon in the first stage of chain folding, encourages subsequent self-assembly of precursor elements.[16,17] PHB creates the initial self-folding chains from random coil at the first stage of the crystallization. After that, the precursor was formed and self-assembled. The reason for this strange behavior of the PHB lamella crystal has not been fully elucidated yet.

Abe et al.[18] investigated the lamella thickness of PHB homopolymer and its copolymers including P(HB-*co*-HHx) (HHx = 8 mol %) by using small-angle X-ray scattering (SAXS). It was found that the lamella thickness of P(HB-*co*-HHx) (HHx = 8 mol %) (1.9 nm) is much thinner than that of

* To whom all correspondence should be addressed. E-mail: hsato@kwansei.ac.jp.
† School of Science and Technology, Kwansei Gakuin University.
‡ Research Center for Environment Friendly Polymers, Kwansei-Gakuin University.
§ Kaneka Corp.
⊥ Graduate School of Engineering, Toyota Technological Institute.
Procter & Gamble Co.

10.1021/ma051777l CCC: $33.50
Published on Web 01/27/2006

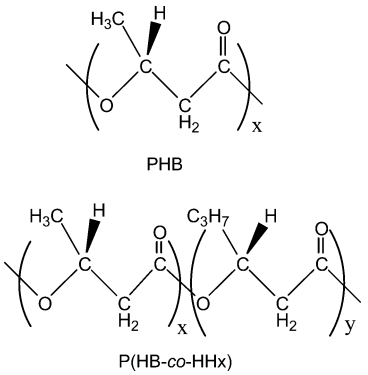

Figure 1. Chemical structures of poly(3-hydroxybutyrate) (PHB) and poly(3-hydroxybutyrate-*co*-3-hydroxyhexanoate) (P(HB-*co*-HHx)).

PHB (5.3 nm). The second monomer units of P(HB-*co*-HHx) are excluded from PHB crystalline lattice, and they may exist mainly on the crystal surface.[19] Therefore, the lattice spacing of P(HB-*co*-HHx) is essentially the same as that of PHB.

To provide new insight into crystallinity and thermal behavior of PHB and P(HB-*co*-HHx), we have been investigating their molecular and crystalline structures by means of wide-angle X-ray diffraction (WAXD),[20] infrared (IR) spectroscopy,[21−25] and differential scanning calorimetry (DSC).[20,23] It was found from temperature-dependent WAXD measurements of PHB and P(HB-*co*-HHx)(HHx = 12 mol %) that the *a* lattice parameter shows the thermal expansion, while the *b* lattice parameter shows very little (P(HB-*co*-HHx)) or a slight change (PHB).[20] It was suggested from this study that there is a particular inter- or intramolecular interaction between the C═O group and the CH_3 group in the PHB and P(HB-*co*-HHx) crystallites and that the interaction becomes weak gradually with temperature along the *a* axis.[20]

In the IR studies[21−25] temperature-dependent IR spectral variations of PHB and P(HB-*co*-HHx) (HHx = 2.5, 3.4, and 12 mol %) allowed us to classify IR bands into the crystalline bands and the amorphous ones. We found that one of the crystalline CH_3 asymmetric stretching bands appears at an anomalously high frequency (3009 cm^{-1}).[21] This observation, together with the results of temperature-dependent WAXD studies and the X-ray crystallographic structure of PHB, led us to conclude that the CH_3 and C═O groups of PHB and P(HB-*co*-HHx) form a C−H···O═C hydrogen bond[26−28] and that a chain of C−H···O═C bonds pair combine the two parallel helical structures.[21,22] The temperature-dependent IR and WAXD studies of PHB and P(HB-*co*-HHx) revealed that the thermal behavior of P(HB-*co*-HHx) (HHx = 12 mol %) is largely different from that of PHB; the crystallinity of P(HB-*co*-HHx) (HHx = 12 mol %) decreases gradually from a fairly low temperature (about 60 °C) while that of PHB changes a little until just below its melting temperature.[20,21]

The present study aims at investigating the importance of C−H···O═C hydrogen bonding in the crystalline and lamella structure and its relation to the thermal behavior of PHB and P(HB-*co*-HHx) (HHx = 2.5, 3.5, 10.5, and 12 mol %) by means of WAXD and IR spectroscopy. The present study is an extension of our previous WAXD and IR studies. In the previous studies we investigated only the heating process of PHB and P(HB-*co*-HHx) (HHx = 12 mol %), but in this study we explore both the heating and cooling processes. In this way we can investigate the reversibility of thermal behavior. The existence and the reversibility of the C−H···O═C hydrogen bonding between the C═O group and the CH_3 group along the *a* axis is explored through the temperature-dependent variations in the *a* and *b* lattice parameters by the WAXD measurements. Moreover, the sizes of the *a* and *b* lattice parameters are compared for PHB and P(HB-*co*-HHx) (HHx = 2.5, 3.4, 10.5, and 12 mol %). The strength and variation of the C−H···O═C hydrogen bonding are analyzed also by temperature-dependent IR spectra in the CH and C═O stretching vibration regions. We have found that there is clear linear relation between the temperature-dependent change in the *a* lattice parameter and that in the CH_3 asymmetric stretching band near 3009 cm^{-1} for PHB and P(HB-*co*-HHx) (HHx = 2.5, 3.4, 10.5, and 12 mol %).

Moreover, in the present study, we estimate the number of the C−H···O═C hydrogen bonding along the *c* axis in the lamella thickness based on the lamella thickness reported by Abe et al.[18] The results for the WAXD and IR studies, together with the estimation of the number of C−H···O═C hydrogen bonding, suggest that the C−H···O═C hydrogen bonding plays an important role in the chain folding of PHB and P(HB-*co*-HHx) with the (110) to ($1\bar{1}0$) (*a* axis) direction. To explain this strange behavior in the chain folding of PHB and P(HB-*co*-HHx), we have modified a proposed model for the lamella crystals of PHB and P(HB-*co*-HHx). In the new model, PHB has a thicker lamella (ca. 5.3 nm) with ca. 9 C−H···O═C hydrogen bondings weakly combining two parallel helical structures, while P(HB-*co*-HHx) (HHx = 10.5 and 12 mol %) has a much thinner lamella (ca. 1.9 nm) with only a few C−H···O═C hydrogen bondings.

Experimental Section

Samples. Bacterially synthesized PHB and P(HB-*co*-HHx) (HHx = 12 mol %) were obtained from the Procter & Gamble Co., Cincinnati, OH. P(HB-*co*-HHx) (HHx = 2.5, 3.5, and 10.5 mol %) were provided by Kaneka Co., Osaka, Japan. They were dissolved in hot chloroform, reprecipitated in methanol as fine powder, and vacuum-dried at 60 °C. Films of PHB and P(HB-*co*-HHx) (HHx = 2.5, 3.4, 10.5, and 12 mol %) were prepared by casting their chloroform solutions on CaF_2 windows. The films were kept in a vacuum-dried oven at 60 °C for 12 h and cooled to room temperature.

Wide-Angle X-ray Diffraction (WAXD). The WAXD data were measured for the precipitated powder samples of PHB and P(HB-*co*-HHx) in the scattering angle range of $2\theta = 4-13°$ by using a two-circle Rigaku X-ray diffractometer equipped with a scintillation detector. Radiation of wavelength 0.710 69 Å (Mo Kα) was employed at generator power of 40 kV and 240 mA. The temperature dependence of the WAXD measurement was controlled by a thermoelectric device (CN4400, OMEGA) with an accuracy of ±0.1 °C. The heating and cooling rates were ca. 1 °C/min.

IR Measurements. The transmission IR spectra were measured at a 2 cm^{-1} resolution using a Thermo Nicolet NEXUS 470 Fourier transform IR spectrometer with a liquid nitrogen cooled mercury−cadmium−telluride detector. A total of 512 scans were coadded for each IR spectral measurement to ensure a high signal-to-noise ratio. The temperature of the IR cell was controlled by a thermoelectric device (CN4400, OMEGA) with an accuracy of ±0.1 °C. The temperature was increased at a rate of ca. 2 °C/min. After changing the temperature, the cell was maintained at that temperature for 15 min to make the samples equilibrate.

Results and Discussion

Difference in the Temperature-Dependent Variations between the *a* and *b* Lattice Parameters. In the present study, we measured temperature-dependent variations in WAXD patterns of P(HB-*co*-HHx) (HHx = 2.5 and 10.5 mol %). The temperature-dependent changes in the WAXD patterns of P(HB-*co*-HHx) (HHx = 2.5 and 10.5 mol %) are very close to those of PHB and P(HB-*co*-HHx) (HHx = 12 mol %) previously

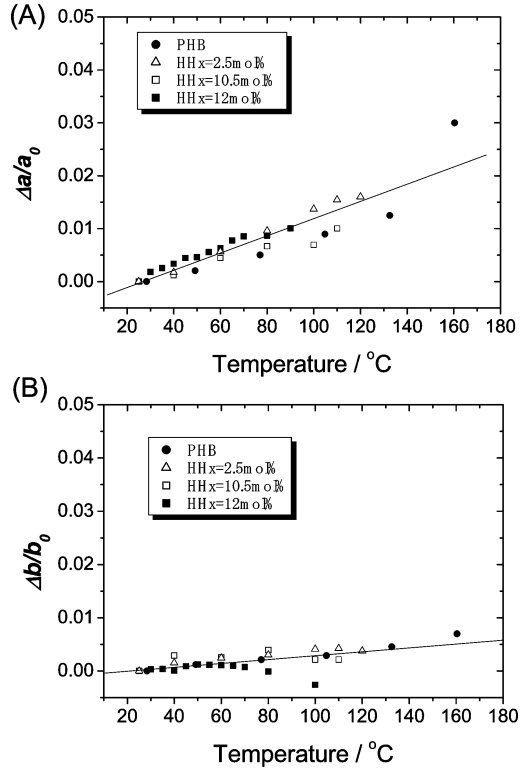

Figure 2. Temperature dependences of (A) $\Delta a/a_0$ and (B) $\Delta b/b_0$ for PHB and P(HB-*co*-HHx) (HHx = 2.5, 10.5, and 12 mol %). a_0 and b_0 are lattice parameters at 25 °C, and Δa (or Δb) is a difference between a_0 (or b_0) and a (or b), the lattice parameter at a particular temperature.

Table 1. Sizes of *a* and *b* Lattice Parameters of PHB and P(HB-*co*-HHx)

	a lattice parameter/Å	*b* lattice parameter/Å
PHB	5.74	13.2
P(HB-*co*-HHx) (HHx = 2.5 mol %)	5.75	13.2
P(HB-*co*-HHx) (HHx = 3.4 mol %)	5.80	13.5
P(HB-*co*-HHx) (HHx = 10.5 mol %)	5.83	13.3
P(HB-*co*-HHx) (HHx = 12 mol %)	5.77	13.3

reported, respectively.[20] Figure 2 plots the temperature dependences of $\Delta a/a_0$ and $\Delta b/b_0$ for PHB and P(HB-*co*-HHx) (HHx = 2.5, 10.5, and 12 mol %). Here, a_0 and b_0 are lattice parameters at 25 °C and Δa (or Δb) are difference between a_0 (or b_0) and the lattice parameters, a (or b), at the temperature measured. It can be clearly seen from Figure 2 that the rates of the increases in the *a* lattice parameters are much faster than those in the *b* lattice parameters and that the *a* lattice parameters increase gradually from room temperature. The thermal coefficients of expansion of the *a* and *b* lattice parameters were estimated to be $(1.6 \pm 0.1) \times 10^{-4}$ and $(3.6 \pm 0.7) \times 10^{-5}$, respectively. Note that the anisotropy of the thermal coefficient of expansion of PHB crystalline is very large.

In our previous study,[20] on the basis of the significant thermal expansion of the *a* lattice parameter, we suggested that there is an intermolecular interaction between the C═O group and the CH_3 group because they are very closely located to each other along the *a* axis.[20] In the present study we have explored the reversibility of the variations in the *a* and *b* lattice parameters as will be discussed later. Moreover, the sizes of *a* and *b* lattice parameters have been compared for PHB and P(HB-*co*-HHx) (HHx = 2.5, 3.4, 10.5, and 12 mol %). Table 1 summarizes the sizes of *a* and *b* lattice parameters of PHB and P(HB-*co*-HHx). It is noted that the size of *a* lattice parameter is the smallest for PHB and increases as the HHx content increases. There may

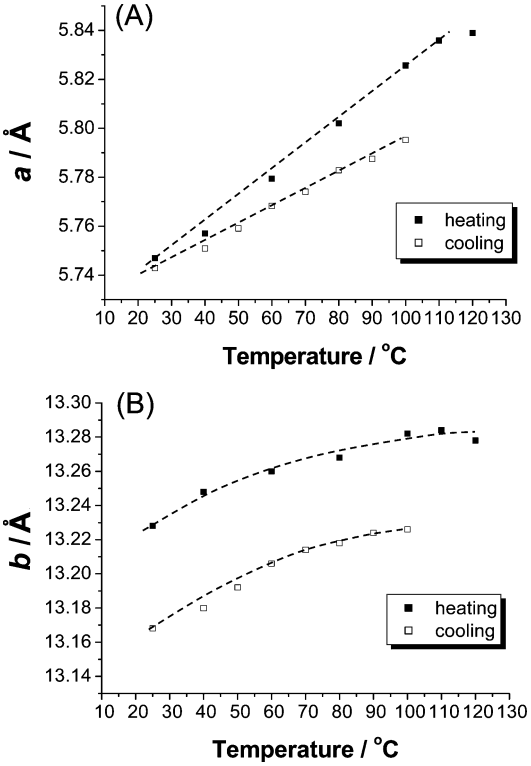

Figure 3. Temperature-dependent variations of the (A) *a* and (B) *b* lattice parameters of P(HB-*co*-HHx) (HHx = 2.5 mol %) in the heating and cooling processes.

be two reasons for this. One is that a few HHx groups enter into the crystal lattice increasing the parameters, although most of them are located out of the lattice. Another is that because of the HHx groups the surface energy destabilizes the total system, leading to the increase in the lattice.

Parts A and B of Figure 3 plot temperature-dependent variations of the *a* and *b* lattice parameters of P(HB-*co*-HHx) (HHx = 2.5 mol %) in the heating and cooling processes, respectively. In the heating process, the increases in the *a* and *b* lattice parameters start from room temperature. It is noted that the values of the *a* lattice parameter at room temperature before the heating process and after the cooling process are almost the same, while the corresponding values of the *b* lattice parameter are significantly different. This result also supports that there are C−H···O═C hydrogen bondings along the *a* axis (not *b* axis). Another interesting point in Figure 3 is that the values of the *a* lattice parameter at higher temperatures in the heating process are much larger than the corresponding ones in the cooling process. For the *b* lattice parameter, the values in the heating process are always larger than those in the cooling process. It is very likely that the crystalline packing of P(HB-*co*-HHx) (HHx = 2.5 mol %) after the first heating process becomes more compact than that before the heating by the heat treatments.

C−H···O═C Hydrogen Bonding and Temperature-Dependent Variations of CH and C═O Stretching Bands of PHB and P(HB-*co*-HHx). In our previous study,[20] we took a new look at the crystal structure of PHB reported by Cornibert and Marchessault[14] and Yokouchi et al.[15] and found that the distance between the O atom of the C═O group and the H atom of the CH_3 group is 2.63 Å, which is shorter than the van der Waals separation (2.72 Å).[21] We also observed the CH_3 asymmetric stretching band of PHB and P(HB-*co*-HHx) (HHx = 2.5, 3.4, and 12 mol %) at an unusually high frequency (~3009 cm^{-1}).[21] On the basis of these two evidences, together

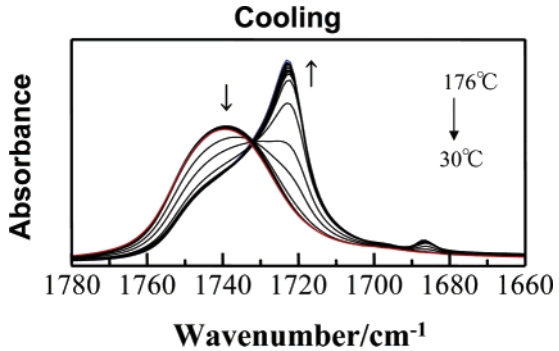

Figure 4. IR spectra in the C═O stretching band region of film of PHB in the cooling process measured over a temperature range of 176−30 °C.

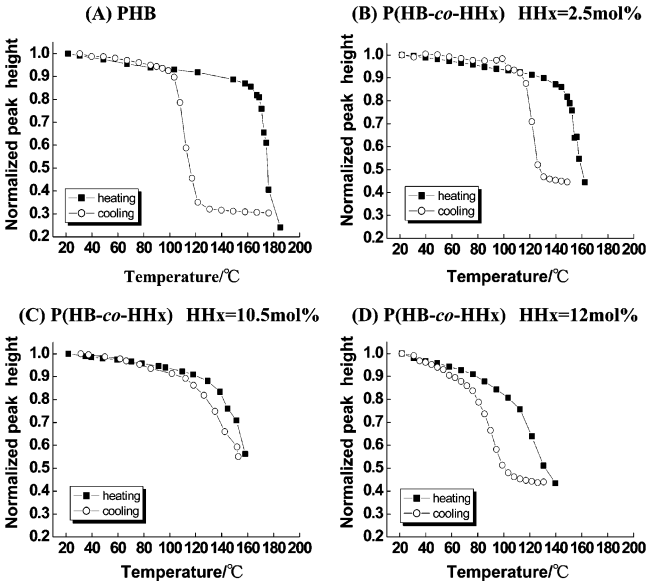

Figure 5. Normalized peak height of the band at 1723 cm^{-1} vs temperature for PHB and P(HB-*co*-HHx) (HHx = 2.5, 10.5, and 12 mol %) in the heating and cooling processes.

with the thermal expansion of the *a* lattice parameter, we proposed that there is an inter- or intra-C−H···O═C hydrogen bonding between the CH_3 group of one helix and the O═C group of another helix in PHB and P(HB-*co*-HHx).[21] In the present study we measured temperature-dependent IR spectral variations of PHB and P(HB-*co*-HHx) (HHx = 2.5, 10.5, and 12 mol %) in both heating and cooling processes. Moreover, the temperature-dependent variations in the *a* lattice parameter are directly compared with those in the wavenumber of the CH_3 asymmetric stretching band.

Figure 4 shows IR spectra in the C═O stretching band region of a film of PHB in the cooling process measured over a temperature range of 176−30 °C. The corresponding spectra for the heating process were reported previously.[21] The trends of the spectral changes are very similar to each other for the heating and cooling processes; however, the changes are not exactly reverse as can been seen later (see Figure 5A). The C═O stretching band region consists of two major bands. One is located at 1723 cm^{-1}. This band decreases in the heating process and eventually disappears at high temperature. In the cooling process, the intensity of this band increases with temperature decrease. This band is assigned to the C═O stretching mode of the crystalline form.[21] The other band is observed near 1740 cm^{-1}. Its intensity increases with temperature in the heating process and decreases in the cooling process. Thus, this band is due to the C═O stretching mode of the amorphous parts.[21] We concluded that the large low-frequency shift of the crystalline C═O stretching bands arises from the formation of C−H···O═C hydrogen bonding.[29]

Thermal behavior and temperature-dependent changes in the C−H···O═C hydrogen bonding of PHB and P(HB-*co*-HHx) can be investigated by monitoring intensity variations of the C═O stretching band at 1723 cm^{-1}. Figure 5A−D plots the normalized peak height of the band at 1723 cm^{-1} vs temperature for PHB and P(HB-*co*-HHx) (HHx = 2.5, 10.5, and 12 mol %) in both heating and cooling processes. It is noted in the comparison of Figure 5A−D that the thermal behavior of P(HB-*co*-HHx) (HHx = 10.5 and 12 mol %) is clearly different from that of PHB and P(HB-*co*-HHx) (HHx = 2.5 mol %) in the both heating and cooling processes. It can be seen from Figure 5C,D that in the heating process the intensity of the C═O stretching band at 1723 cm^{-1} decreases gradually from a fairly low temperature for P(HB-*co*-HHx) (HHx = 10.5 and 12 mol %). This indicates that the crystalline states of P(HB-*co*-HHx) (HHx = 10.5 and 12 mol %) deform gradually from a fairly low temperature, which is much lower than their melting temperatures. Figure 5C,D also reveals that in the cooling process the formation of the crystallines begins from a fairly high temperature and proceeds gradually. In contrast to P(HB-*co*-HHx) (HHx = 10.5 and 12 mol %), in the heating process of PHB and P(HB-*co*-HHx) (HHx = 2.5 mol %) (Figure 5A,B) the intensity of the C═O stretching band changes little until just below their melting temperature.[21] In the cooling processes of PHB and P(HB-*co*-HHx) (HHx = 2.5, 10.5, and 12 mol %) they show a hysteresis curve; the crystallization starts at a much lower temperature than the melting temperature. The temperature where the crystallization starts is very close to T_c (PHB, 108 °C; HHx = 2.5 mol %, 113 °C; HHx = 10.5 mol %, 114 °C; and HHx = 12 mol %, 80 °C). It is also noted that the crystallization of PHB and P(HB-*co*-HHx) (HHx = 2.5, 10.5, and 12 mol %) happens at a much faster rate than that of P(HB-*co*-HHx) (HHx = 10.5 and 12 mol %). Therefore, the IR results together with the results for WAXD[20] suggest that if the HHx content becomes large (probably more than 10 mol %), the thermal behavior changes dramatically, and the crystallinity decreases gradually from a low temperature.

Parts A and A′ of Figure 6 ′ show IR spectra in the 3050−2900 cm^{-1} region and their second derivatives of PHB in the cooling process measured over a temperature range of 176 to 30 °C, respectively. The corresponding spectra for the heating process were reported in our previous paper.[21] The band assignments in the 3050−2900 cm^{-1} region are still not clear, but there is little doubt that the band at 3009 cm^{-1} (Figure 6) is due to the CH_3 asymmetric stretching band.[21] We assigned this band to the C−H stretching (pseudo-CH_3 asymmetric stretching) mode of the C−H···O═C hydrogen bonding because this band shows a significant higher wavenumber shift compared with the frequency for the amorphous band (2984 cm^{-1}).[21]

It can be seen from Figure 6A′ that the CH stretching band at 3009 cm^{-1} of PHB shows a gradual high-frequency shift with the intensity increase. In the heating process the corresponding band shows a gradual low-frequency shift with temperature, but its intensity changes a little.[21] The trends of temperature-dependent spectral variations are very close to each other for the heating and cooling processes, but the variations are not exactly reverse as can be seen later (Figure 8A). The corresponding CH stretching band of P(HB-*co*-HHx) (HHx = 10.5 and 12 mol %) becomes weak from a fairly low temperature with a lower wavenumber shift in the heating process. These observations indicate that the C−H···O═C hydrogen bonding

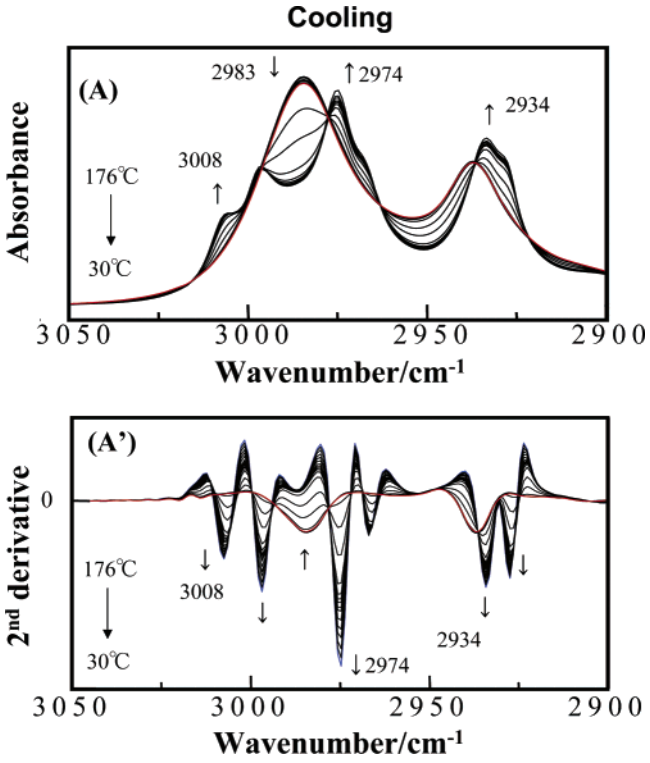

Figure 6. (A, A′) IR spectra in the 3050−2900 cm^{-1} region and their second derivatives of PHB measured in the cooling process over a temperature range of 176−30 °C.

becomes weak but does not break down until just below the melting temperature in PHB, but it becomes weak and breaks gradually from the fairly low temperature in P(HB-*co*-HHx) (HHx = 10.5 and 12 mol %).

Parts A and B of Figure 7 show temperature-dependent variations of the wavenumber of the CH stretching band at 3009 cm^{-1} for PHB and P(HB-*co*-HHx) (HHx = 2.5, 3.4, 10.5, and 12 mol %) in the heating and cooling processes, respectively. Figure 8A−D illustrates the corresponding variations of the peak height at 3009 cm^{-1} in the second derivatives for PHB and P(HB-*co*-HHx) (HHx = 2.5, 10.5, and 12 mol %). It is noted in Figure 7A that among PHB and P(HB-*co*-HHx) (HHx = 2.5, 3.4, 10.5, and 12 mol %) the CH stretching band of PHB has the highest frequency, and as the HHx content increases, the wavenumber decreases; P(HB-*co*-HHx) (HHx = 12 mol %) yields the lowest wavenumber. These results suggest that the strength of the C−H···O═C bonding is strongest in PHB, and it becomes weaker as the HHx content becomes larger. This conclusion corresponds well to the fact that the *a* and *b* lattice parameters are shortest in PHB, and they become larger when more HHx are involved in the copolymers. Figure 9 plots the frequency of the CH stretching band vs a lattice parameter for PHB and P(HB-*co*-HHx) (HHx = 2.5, 10.5, and 12 mol %). The results in Figure 9 suggest that as temperature increases, the *a* lattice parameter increases and the C−H···O═C hydrogen bonding becomes weak. Of note in Figure 8 is that the temperature-dependent changes in the peak height of the CH stretching band at 3009 cm^{-1} are in parallel with those of the C═O stretching band at 1723 cm^{-1} in both heating and cooling processes (Figure 5).

Differences in the Crystalline and Lamella Structures between PHB and P(HB-*co*-HHx) (HHx = 10.5 and 12 mol %). On the basis of the above WAXD and IR studies, we propose models for the crystalline structure (lamella) of PHB and P(HB-*co*-HHx) (HHx = 10.5 and 12 mol %); see Figure

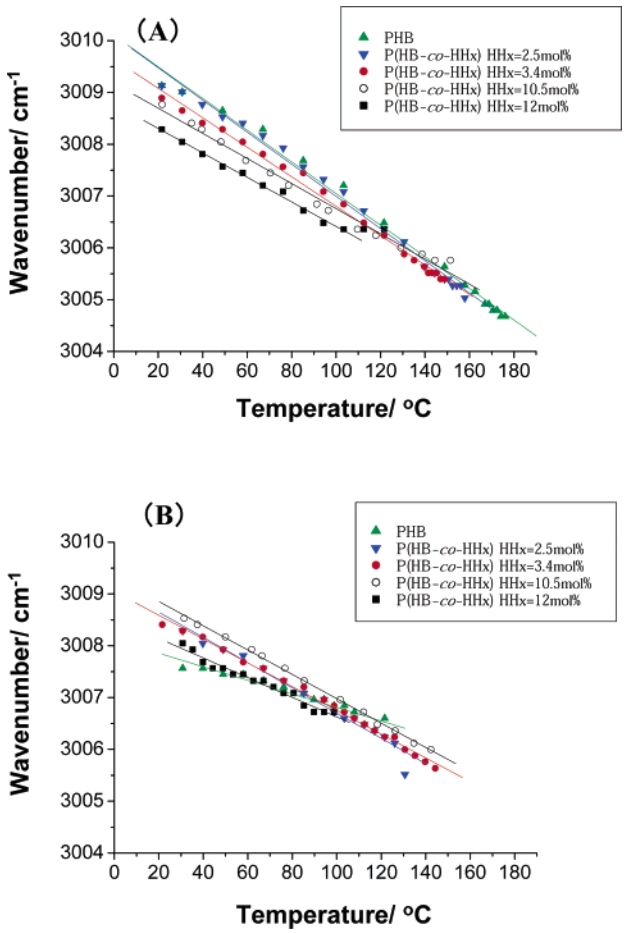

Figure 7. Temperature-dependent variations of the wavenumber of the CH stretching band at 3009 cm^{-1} for PHB and P(HB-*co*-HHx) (HHx = 2.5, 3.4, 10.5, and 12 mol %) in the (A) heating and (B) cooling processes.

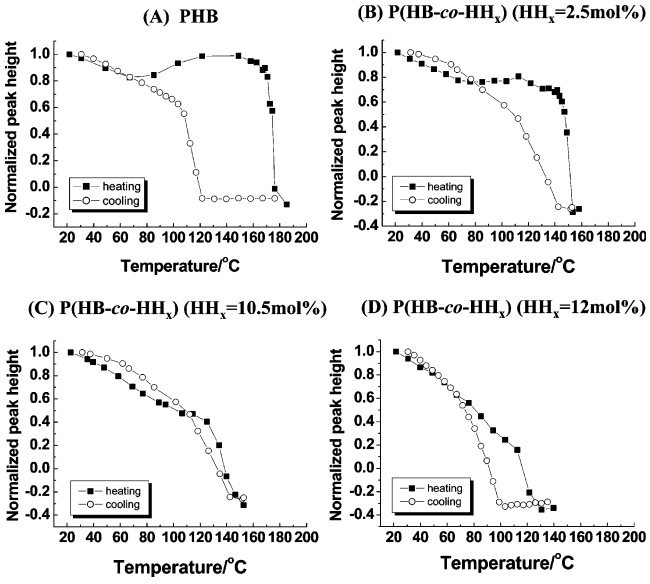

Figure 8. Temperature-dependent variations of the peak height of the CH stretching band at 3009 cm^{-1} in the second derivatives in the (■) heating and (○) cooling processes for PHB and P(HB-*co*-HHx) (HHx = 2.5, 10.5, and 12 mol %).

10. These models are based on the lamella structure proposed by Iwata et al.[19] and the lamella thickness of PHB and P(HB-*co*-HHx) (HHx = 8 mol %) determined by Abe et al.[18] by means of SAXS. Abe et al.[18] found that the lamella thickness of P(HB-*co*-HHx) (HHx = 8 mol %) (1.9 nm) is much thinner than that

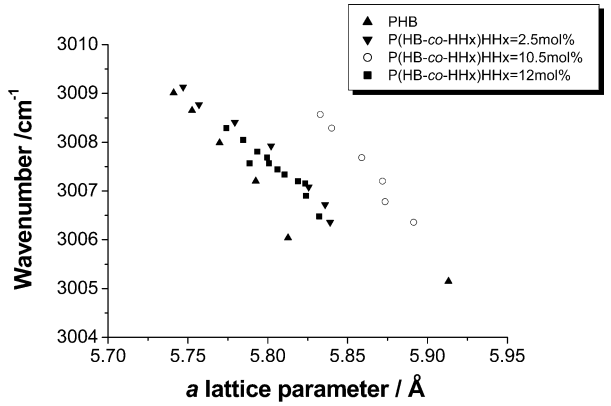

Figure 9. Frequency of CH stretching band near 3008 cm^{-1} vs the size of *a* lattice parameter for PHB and P(HB-*co*-HHx) (HHx = 2.5, 10.5, and 12 mol %).

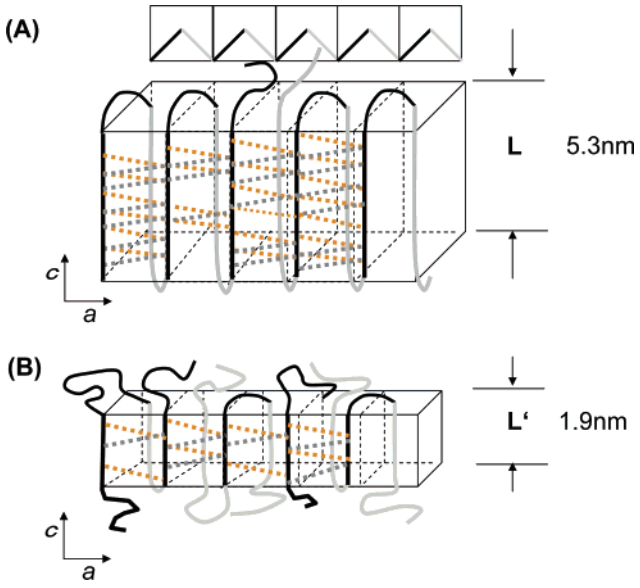

Figure 10. Proposed models for the lamella structure of (A) PHB and (B) P(HB-*co*-HHx) (HHx = 10.5 and 12 mol %).

of PHB (5.3 nm) at the same crystallization temperature (60 °C). The differences in the lamella thickness and surface structure of these crystalline depend on the amount of the second monomer unit (HHx in the present case). The HHx part probably does not form crystalline structure and comes out of the surface. Thus, the lamella thickness of P(HB-*co*-HHx) copolymers is thinner than that of PHB homopolymer, even if the HHx content is small.

We have estimated the number of the CH···O═C hydrogen bonding along the *c* axis in the lamella thickness of PHB and P(HB-*co*-HHx) (HHx = 10.5 and 12 mol %) by using the reported lamella thickness. For the lamella thickness of P(HB-*co*-HHx) (HHx = 10.5 and 12 mol %), we have used that of P(HB-*co*-HHx) (HHx = 8 mol %) because the former is not available. The number of CH···O═C hydrogen bonding of PHB has been estimated to be about 8 or 9, while that of P(HB-*co*-HHx) (HHx = 10.5 and 12 mol %) is about 3. There is a large difference in the number of the CH···O═C hydrogen bonding between PHB and the P(HB-*co*-HHx) copolymers because PHB has nearly perfect crystalline structure, while P(HB-*co*-HHx) has a relatively large amount of amorphous parts due to the HHx contents. Therefore, the CH···O═C hydrogen bonding may break much more easily in P(HB-*co*-HHx) (HHx = 10.5 and 12 mol %). It seems that the C−H···O═C hydrogen bondings combine two parallel helical chains along the *a* axis, stabilizing the peculiar chain folding of PHB and P(HB-*co*-HHx). The quite different thermal behavior between PHB and P(HB-*co*-HHx) (HHx = 10.5 and 12 mol %) may be understood from the models shown in Figure 10. However, one must notice that the apparent crystallinity of P(HB-*co*-HHx) is still high (ca. 35%) even if the HHx content is more than 10 mol %.[18] The crystallinity of linear low density polyethylene drops suddenly even if the content of short branches is only about several mol %.[30] Since P(HB-*co*-HHx) is a random copolymer, P(HB-*co*-HHx) (HHx = 10 mol %) means that the probability of finding two consecutive units of 3HB is 0.9^2. In fact, the probability of finding *n* consecutive units of 3HB without the disruption by HHx is simply 0.9^n. This suggests that the probability of finding a segment without the HHx group is smaller than the probability of having at least one HHx defect, when *n* is greater than seven. Therefore, it may be concluded that the P(HB-*co*-HHx) crystal lamella consists of only a few turns of helix but still keeps a lamella structure probably because the C−H···O═C hydrogen bonding combines the two parallel helices. Therefore, P(HB-*co*-HHx) shows the apparent high crystallinity even if it has the HHx content of more than 10 mol %.

Conclusion

The present study has aimed at exploring the relation between the crystal and lamella structure of PHB and P(HB-*co*-HHx) and C−H···O═C hydrogen bonding. We have reached two important conclusions. One is that the formation of C−H···O═C hydrogen bonding stabilizes the chain folding in the lamella structure of PHB and P(HB-*co*-HHx), and the other is that the high crystallinity of PHB and P(HB-*co*-HHx) partly comes from the C−H···O═C hydrogen bonding.

In the temperature dependence of X-ray diffraction of P(HB-*co*-HHx) (HHx = 2.5, 3.4, 10.5, and 12 mol %), it was found that the thermal expansion is much larger in the *a* lattice parameter than in the *b* lattice parameter and that the values of the *a* lattice parameter at room temperature before the heating process and after the cooling process are almost the same while the value of the *b* lattice parameter varies. It was found that the variations in only the *a* lattice parameters show reversibility during the heating and cooling processes of PHB and P(HB-*co*-HHx). The CH stretching band of the hydrogen-bonded CH_3 group appears near 3009 cm^{-1} for PHB and P(HB-*co*-HHx) (HHx = 2.5, 10.5, and 12 mol %), and this wavenumber becomes lower when the *a* lattice parameter becomes larger. Therefore, when the *a* lattice parameter is larger (P(HB-*co*-HHx) (HHx = 10.5 and 12 mol %), the C−H···O═C hydrogen bonding is weaker.

The difference in the lamella structure between PHB and P(HB-*co*-HHx) arises from the second monomer unit, HHx. We have proposed the model structure for the lamella of PHB and P(HB-*co*-HHx) (HHx = 10.5 and 12 mol %). The number of the C−H···O═C hydrogen bonding was estimated to be ca. 8−9 and ca. 3, respectively, for PHB and P(HB-*co*-HHx) (HHx = 10.5 and 12 mol %). It is very likely that the C−H···O═C hydrogen bonding plays an important role in stabilizing the peculiar chain folding in PHB and P(HB-*co*-HHx).

Acknowledgment. The authors thank Prof. Tadahisa Iwata (RIKEN) for valuable discussion. This work was partially supported by "Open Research Center" project for private universities: matching fund subsidy from MEXT (Ministry of Education, Culture, Sports, Science and Technology), 2001−2005. This work was supported also by Kwansei-Gakuin University "Special Research" project, 2004−2008.

References and Notes

(1) Lemoigne, M. *Bull. Soc. Chim. Biol.* **1926**, *8*, 770.
(2) Doi, Y. *Microbial Polyesters*; VCH Publishers: New York, 1990.
(3) Vert, M. *Biomacromolecules* **2005**, *6*, 538.
(4) Chiellini, E.; Solaro, R. *Recent Advances in Biodegradable Polymers and Plastics*; Wiley-VCH: Weinheim, 2003.
(5) Doi, Y. *ICBP 2003 First IUPAC International Conference on Bio-Based Polymers*; *Macromolecular Bioscience*, Vol. 4, Issue 3; Wiley-VCH: Weinheim, 2004.
(6) Bastioli, C. *Handbook of Biodegradable Polymers*; Rapra Technology Limited: UK, 2005.
(7) Satkowski, M. M.; Melik, D. H.; Autran, J.-P.; Green, P. R.; Noda, I.; Schechtman, L. A. In *Biopolymers*; Steinbüchel, A., Doi, Y., Eds.; Wiley-VCH: Wienhiem, 2001; p 231.
(8) Iwata, T.; Aoyagi, Y.; Fujita, M.; Yamane, H.; Doi, Y.; Suzuki, Y.; Takeuchi, A.; Uesugi, K. *Macromol. Rapid Commun.* **2004**, *25*, 1100.
(9) Doi, Y.; Kitamura, S.; Abe, H. *Macromolecules* **1995**, *28*, 4822.
(10) Kobayashi, G.; Shiotani, T.; Shima, Y.; Doi, Y. In *Biodegradable Plastics and Polymers*; Doi, Y., Fukuda, K., Eds.; Elsevier: Amsterdam, 1994; p 410.
(11) Web site: www.nodax.com.
(12) Kunioka, M.; Tamaki, A.; Doi, Y. *Macromolecules* **1989**, *22*, 694.
(13) Yoshie, N.; Saito, M.; Inoue, Y. *Polymer* **2004**, *45*, 1903.
(14) Cornibert, J.; Marchessault, R. H. *J. Mol. Biol.* **1972**, *71*, 735.
(15) Yokouchi, M.; Chatani, Y.; Tadokoro, H.; Teranishi, K.; Tani, H. *Polymer* **1973**, *14*, 267.
(16) Marchessault, R. H.; Yu, G. In *Biopolymers, Polyesters II*; Doi, Y., Steinbüchel, A., Eds.; Wiley-VCH: Wienhiem, 2002; p 157.
(17) Marchessault, R. H.; Kawada, J. *Macromolecules* **2004**, *37*, 7418.
(18) Abe, H.; Doi, Y.; Aoki, H.; Akehata, T. *Macromolecules* **1998**, *31*, 1791.
(19) Iwata, T.; Shiromo, M.; Doi, Y. *Macromol. Chem. Phys.* **2002**, *203*, 1309.
(20) Sato, H.; Nakamura, M.; Padermshoke, A.; Yamaguchi, H.; Terauchi, H.; Ekgasit, S.; Noda, I.; Ozaki, Y. *Macromolecules* **2004**, *37*, 3763.
(21) Sato, H.; Murakami, R.; Padermshoke, A.; Hirose, F.; Senda, K.; Noda, I.; Ozaki, Y. *Macromolecules* **2004**, *37*, 7203.
(22) Sato, H.; Dybal, J.; Murakami, R.; Noda, I.; Ozaki, Y. *J. Mol. Struct.* **2005**, *744*−*747*, 35.
(23) Sato, H.; Padermshoke, A.; Nakamura, M.; Murakami, R.; Hirose, F.; Senda, K.; Terauchi, H.; Ekgasit, S.; Noda, I.; Ozaki, Y. *Macromol. Symp.* **2005**, *220*, 123.
(24) Padermshoke, A.; Sato, H.; Katsumoto, Y.; Ekgasit, S.; Noda, I.; Ozaki, Y. *Vib. Spectrosc.* **2004**, *36*, 241.
(25) Padermshoke, A.; Katsumoto, Y.; Sato, H.; Ekgasit, S.; Noda, I.; Ozaki, Y. *Polymer* **2004**, *45*, 6547.
(26) Desiraju, G. R.; Steiner, T. *The Weak Hydrogen Bond in Structural Chemistry and Biology*; Oxford University Press: New York, 1999; pp 29−121.
(27) Matsuura, H.; Yoshida, H.; Hieda, M.; Yamanaka, S.; Harada, T.; Shinya, K.; Ohno, K. *J. Am. Chem. Soc.* **2003**, *125*, 13910.
(28) Hobza, P.; Havlas, Z. *Chem. Rev.* **2000**, *100*, 4253.
(29) Zhang, J.; Sato, H.; Tsuji, H.; Noda, I.; Ozaki, Y. *J. Mol. Struct.* **2005**, *735*−*736*, 249.
(30) Kroschwitz, J. I. *Concise Encyclopedia of Polymer Science and Engineering*; John Wiley & Sons: New York, 1990; pp 350−357.

MA051777L